Use of UAV imagery for the detection and measurement of damages to road networks in landslide areas

Nappo, Nicoletta; Mavrouli, Olga; Núñez-Andrés, Maria Amparo

DOI
10.1016/B978-0-12-823868-4.00017-9

Publication date
2024

Document Version
Final published version

Published in
Earth Observation Applications to Landslide Mapping, Monitoring and Modeling

CHAPTER SIXTEEN

Use of UAV imagery for the detection and measurement of damages to road networks in landslide areas

Nicoletta Nappo[1,2], Olga Mavrouli[3] and Maria Amparo Núñez-Andrés[4]
[1]Department of Geoscience & Engineering, Delft University of Technology, Delft, The Netherlands
[2]Deltares, Delft, The Netherlands
[3]Department of Civil Engineering, University of West Attica, Athens, Greece
[4]Department of Civil and Environmental Engineering, Universitat Politècnica de Catalunya-Barcelona Tech, Barcelona, Spain

Introduction

Public administrative organizations and private companies managing road infrastructure face the challenge of deteriorating road network assets either due to usual stresses (e.g., vehicle loadings, traffic incidents, weathering) or because of exceptional causes such as earthquakes and slope instabilities, causing disruption and loss of functionality of the infrastructure (AASHO, 1962; ANAS, 2004; ASTM, 2020; Mavrouli et al., 2019; Nappo et al., 2021; Postance et al., 2017). Landslides, in particular, result in billions spent globally for the repair of severe road destructions or small-scale pavement anomalies. The correlation of pavement damage (effect) with the intensity of the ground movement (cause) provides road vulnerability, which is of utmost importance to mitigating landslide risks and achieving safe and resilient transport networks (Achillopoulou et al., 2020). Moreover, increasing patterns of road deformation in time may serve as premonitory signs of larger failures. To this end, the monitoring of road pavement damage is essential in landslide-affected areas.

Different approaches exist for monitoring the condition of linear infrastructures during their service life. The majority of roadway maintenance strategies are based on the assessment of the structural and operational performance of the road pavements under usual stresses using the Pavement Condition Index, the Pavement Serviceability Index, and the International Roughness Index (IRI) (ANAS, 2004; ASTM, 2015; ASTM, 2020; Bryce et al., 2019; Elhadidy et al., 2021; George et al., 1989; Hatmoko et al., 2019; Park et al., 2007; Radopoulou et al., 2016; Sidess et al., 2021; Zhang & Wang, 2018). On the other hand, particularly for landslide-affected roads, the relatively limited existing scientific research has been addressing the vulnerability of road infrastructure to slope instabilities (Mavrouli et al., 2019; Pantelidis, 2011), slow-moving

Earth Observation Applications to Landslide Mapping, Monitoring and Modeling.
DOI: https://doi.org/10.1016/B978-0-12-823868-4.00017-9

landslides (Mansour et al., 2011; Postance et al., 2017), debris flows (Winter et al., 2013; Winter et al., 2016), earthquakes (Anbazhagan et al., 2012) or their combination (Achillopoulou et al., 2020; Argyroudis et al., 2019; Argyroudis et al., 2020).

The assessment of road vulnerability and the reconstruction of damage evolution over time remain crucial points under research and a challenge, as they require damage data for varying hazard intensities and over time. The severity of road pavement damage due to landslides is commonly expressed as a function of roadway blockage (Winter et al., 2013; Winter, 2019), human losses (Petrucci & Gullà, 2010), road repair costs (Donnini et al., 2017; Mavrouli et al., 2019), landslide movement rate (Mansour et al., 2011; Mavrouli et al., 2019) or landslide-induced differential displacements of the road pavement (Ferlisi et al., 2021; Nappo et al., 2019). The classification of the severity of road damage caused by landslides using a road-related proxy such as pavement roughness (i.e., IRI) has been suggested by (Nappo et al., 2021). Subjectivity in the evaluations, incomplete inventories, or requirements of expensive instrumentations in order to have extensive data are making the quantification of pavement damage a difficult task. Nevertheless, nowadays, techniques such as close-range digital photogrammetry (DP) using Unmanned Aerial Vehicles (UAVs) can be used for extracting detailed records of the damage, given that adequate methodologies are being developed for this aim.

This chapter reviews the techniques adopted in the scientific literature for road damage detection and measurement in landslide areas, with a specific focus on the use of photogrammetry from UAVs and the methodologies for data processing. Examples from the existing literature are presented here to discuss the advantages and disadvantages of using this technique for road damage characterization, compared to other methods. The aim is to determine which techniques, products, and processing methodologies are suitable for fine to coarse-scale analyses of road damage due to landslides.

Road deformation monitoring: from in-situ measurements to remote sensing techniques

The extent of road damage is usually presented in terms of road displacements or deformation or deposited soil-rock volume causing the road blockage, depending on the landslide type.

For a local or detailed scale of analysis, visual inspections are a traditional way of evaluating the condition of the road infrastructure and determining the typology of pavement damage recurring in landslide areas. For in situ monitoring, inclinometers and extensometers have also been proved useful to provide the damage extent as associated with the measured displacements (Mavrouli et al., 2019). More recently, advances in Interferometric Synthetic Aperture Radar (InSAR) techniques have allowed estimating the displacement

and deformation pattern on road networks induced by subsidence (Cigna et al., 2017; Orellana et al., 2020; Ponzo et al., 2021) and landslides (Ferlisi et al., 2021; Macchiarulo et al., 2022; Nappo et al., 2019). Although the widespread usage of InSAR data for computing landslide-induced (differential) displacements affecting the pavement of different road networks, such technique presents limitations for detecting and characterizing road pavement cracking, depression, or upheaval commonly caused by landslides (ANAS, 2004; ASTM, 2015; Mavrouli et al., 2019; Nappo et al., 2021). For this reason, alternative or complementary techniques and technologies need to be considered.

Since the 2000s, first Terrestrial and later Mobile Laser Scanners (TLS and MLS) were introduced for inspecting road conditions (Coenen & Golroo, 2017; Mertz, 2011; Ragnoli et al., 2018). Nowadays, UAVs with mounted image sensors allow us to incorporate DP into the methods for detecting and measuring pavement damage (Inzerillo et al., 2018; Nappo et al., 2021). Along the same line, innovations in computer vision algorithms seem promising for the assessment of the condition of roadways (Gharaibeh & Lindholm, 2014) and the inspection of pavement damage (Cubero-Fernandez et al., 2017; Nhat-Duc et al., 2018; Oliveira & Correia, 2013; Wang et al., 2019).

Sensors for assessing road damage and condition

Two groups of sensors acquiring different types of information can be distinguished: digital cameras for acquiring 2D images of the road pavement, and laser sensors that provide directly a 3D point cloud model. The images can be processed via computer vision algorithms to detect geometrical features and anomalies such as cracks. Moreover, if the images are acquired so that they comply with the principles of stereophotogrammetry (i.e., considering adequate overlap and changes in the point of view), a 3D surface model of the road can be built.

Digital cameras as being accessible and affordable devices have been widely adopted by road agencies to corroborate the condition of the road infrastructure during field surveys and visual inspections (Nappo et al., 2021; Ragnoli et al., 2018; Wang & Gong, 2002; Wang & Li, 1999). The same typology of digital images, which are acquired in the visible spectrum of light, can be processed using a variety of image analysis algorithms to extract pavement features and distresses. Binarization and thresholding (Cubero-Fernandez et al., 2017; Oliveira & Correia, 2009; Powell & Satheeshkumar, 2017; Puan et al., 2007; Zou et al., 2012), edge detection (Canny, 1986; Mancini et al., 2013; Zou et al., 2012), morphological operators (Cubero-Fernandez et al., 2017; Mathavan et al., 2014), Markov random field (Chambon et al., 2009), fuzzy logic (Mancini et al., 2013), convolutional neural networks (CNN) (Mandal et al., 2019; Nhat-Duc et al., 2018) and deep learning (Mathavan, Rahman, et al., 2015) are processing algorithms proposed in the scientific literature to extract road pavement distress

features from 2D digital images with high accuracy, often exceeding 95% (Chambon & Moliard, 2011; Coenen & Golroo, 2017; Mathavan, Kamal, et al., 2015; Nappo et al., 2021; Ragnoli et al., 2018; Wang et al., 2019; Zakeri et al., 2017). Possible occlusions due to the perspective are a shortcoming of these techniques. So far, image processing is performed by researchers rather than road maintenance authorities and practitioners.

TLS adopt LiDAR (Light Detection And Ranging) technology to acquire the spatial coordinates of 3D objects by emitting a laser pulse toward the target and measuring the distance between the device and the target (Vosselman & Maas, 2010). The accuracy of most TLS sensors ranges between 3 and 6 mm @100 m and varies proportionally with distance from the target, thus allowing scientists and road agencies to investigate either limited portions of the road pavement or entire infrastructure assets (Oguchi et al., 2011; Ragnoli et al., 2018; Vosselman & Maas, 2010). The measures of road pavement unevenness obtained with TLS are comparable with IRI values obtained with traditional precision levels and laser profilometers (Chin, 2012; Ragnoli et al., 2018). The main drawback of using TLS for road damage assessment is the necessity of multiple acquisitions from different positions to reconstruct the 3D model of a consistent portion of the roadway (Tan & Li, 2019) avoiding occlusions and hidden areas.

MLS are mounted on moving vehicles and reconstruct continuous 3D models by acquiring single or multiple scans of the investigated target (Ragnoli et al., 2018; Schnebele et al., 2015; Williams et al., 2013). This technique is particularly useful for pavement surface acquisitions, with an accuracy of about 1 cm depending on the speed of the hosting vehicle (Cahalane et al., 2016; Ragnoli et al., 2018; Williams et al., 2013). Disadvantages of MLS are the necessity of multiple acquisitions over the same area to reconstruct the model of the entire width of the roadway, and the slowdown of traffic flow due to the limited speed of the vehicles hosting the sensor (Tan & Li, 2019). Moreover, to coregister the different acquisitions, differential Global Navigation Satellite System (GNSS) and Inertial Measurement Unit sensors are necessary.

UAVs have been emerging in the last two decades as a low-cost alternative platform to airplanes or helicopters to acquire images and reconstruct 3D point clouds of the investigated target with centimetric accuracy and low computational time (Nex & Remondino, 2014; Nex et al., 2022; Remondino et al., 2017; Schnebele et al., 2015). Three types of UAV are available: fixed-wing, rotorcraft, and vertical take-off and landing vehicles (Greenwood et al., 2019). The major advantage of using UAVs for road damage assessment is the possibility of surveying risky or inaccessible locations (Tahar, 2013). Other advantages are the shorter acquisition time and the maneuverability of the aircraft that allows moving along or around the target for better and more detailed acquisitions.

Table 16.1 provides examples from the scientific literature of the applications of TLS, MLS, and DP from UAVs for condition assessment and damage detection on road pavements and bridges, inspection of roadway tunnels, and feature recognition of other infrastructure assets (e.g., traffic signs, poles, guardrail and retaining walls).

Table 16.1 Examples of use of Terrestrial and Mobile Laser Scanner (TLS and MLS) and digital photogrammetry (DP) from Unmanned Aerial Vehicles (UAV) for monitoring road infrastructure components.

Road infrastructure component	Application	Technique	References
Pavement	Condition assessment	TLS	Alhasan et al. (2017); Barbarella et al. (2018)
		MLS	Cahalane et al. (2016); Díaz-Vilariño et al. (2016); Kumar and Angelats (2017)
		DP_UAV	Cardenal et al. (2019); Gomez and Purdie (2016); Greenwood et al. (2019)
	Damage detection	TLS	Akgul et al. (2017); Ouyang and Xu (2013); Uddin (2014)
		MLS	De Blasiis et al. (2020); Kumar et al. (2015); Van Der Horst et al. (2019)
		DP_UAV	Inzerillo et al. (2018); Nappo et al. (2021); Saad and Tahar (2019); Tan and Li (2019)
Bridge	Condition assessment	TLS	Guldur et al. (2015); Lõhmus et al. (2018); Matsumoto et al. (2018)
		DP_UAV	Chen et al. (2019); Pan et al. (2019)
	Damage detection	TLS	Liu et al. (2019); Sedek and Serwa (2016); Valença et al. (2017)
		DP_UAV	Lei et al. (2018)
Tunnel	Inspection	TLS	Argüelles-Fraga et al. (2013)
Other assets (e.g., traffic signs, poles, guardrails, retaining walls)	Feature recognition	TLS	Barbarella et al. (2019)
		MLS	Guan et al. (2015); Holgado-Barco et al. (2017); Li et al. (2018)

UAV platforms for pavement damage assessment in landslide-affected areas

The advent of UAV in cartography (Crommelinck et al., 2017; James et al., 2017; Pagán et al., 2019; Santise et al., 2014; Tahar, 2013), landslide monitoring (Casagli et al., 2017; Fazio et al., 2019; Lissak et al., 2020; Niethammer et al., 2011) and structural damage assessment (Fernandez Galarreta et al., 2015; Nex et al., 2019; Stumpf et al., 2013; Vetrivel et al., 2018) among others, can be mainly attributed to their capacity of collecting high-resolution images of the investigated target avoiding hidden zones and being near hazardous areas that are otherwise hardly accessible.

UAV platforms can be equipped with digital and multispectral cameras, LiDAR, thermal detectors and other sensors, depending on their field of application (Giordan et al., 2020; Nex et al., 2022; Tahar, 2013), and data can be acquired from different altitudes (i.e., from close- to long-range with the limit fixed by the rules in each country or region) and in different directions (i.e., nadir or oblique geometry) (Fernández-Hernandez et al., 2015; Martínez-Carricondo et al., 2018; Nex & Remondino, 2014). Data acquisition can be performed manually, semiautonomously, or autonomously depending on the degree of intervention of the UAV operator (Tahar, 2013). RGB digital cameras are the most common sensor due to the advances in photogrammetry and computer vision that allow RGB image data to be employed either for 2D investigations (e.g., mapping, deep learning, semantic scene analysis) or 3D scene reconstruction and analysis (Giordan et al., 2020; Martínez-Carricondo et al., 2018; Nex & Remondino, 2014; Nex et al., 2022).

The most common techniques for processing 2D digital images have been presented in Section 3. As for the 3D scene reconstruction, currently, structure from motion (SfM) is the most used algorithm that allows the processing of a sequence of 2D images to reconstruct sparse and dense point clouds of the target (Giordan et al., 2020; Martínez-Carricondo et al., 2018; Nex & Remondino, 2014). This algorithm automatically identifies and matches corresponding features in different images, and then creates a network of tie points determining their 3D coordinates, thus generating a 3D point cloud (James et al., 2017; Lucieer et al., 2014; Snavely et al., 2008; Vasuki et al., 2014; Westoby et al., 2012). From this 3D model, the images can be orthoprojected to obtain other useful products, such as the orthophoto of the surveyed scene or target (Giordan et al., 2020; Nex & Remondino, 2014; Westoby et al., 2012). Optimal results are obtained when the sequence of target images has a minimum overlap of 80% (Nex & Remondino, 2014). The main advantage of SfM is the possibility of automatically calculating the camera parameters, camera position and orientation, and geometry of the scene (Giordan et al., 2020; Martínez-Carricondo et al., 2018; Westoby et al., 2012). The generated 3D model can be returned in relative or absolute coordinates, depending on the georeferencing system.

Ground control points (GCPs), onboard GNSS (absolute position or real-time kinematic [RTK] network), and GNSS ground reference systems (post processing kinematic [PPK] or RTK) can be used to determine the coordinates in a global system of the output model (Caroti et al., 2015; Giordan et al., 2020; Martínez-Carricondo et al., 2018). The overall accuracy of the 3D point cloud and the 2D orthophoto depends on the internal sensor characteristics, the accurate flight plan, the use of GCPs, and the georeferencing system (Caroti et al., 2015). The accuracy of UAV-based photogrammetric products is commonly assessed using the root mean square error (RMSE) achieved after the bundle adjustments of all the images in the SfM method (Caroti et al., 2015; Martínez-Carricondo et al., 2018). Despite the popularity

of UAVs in engineering geology studies and infrastructure condition assessment, the use of this technique for road damage characterization in landslide areas is still limited (Nappo et al., 2021). The few available studies adopt UAV-based 3D models to (semi) automatically detect potholes or block cracks on the road pavement that are typically caused by a poor mixture of asphalt components and water infiltration, rather than landslides (ASTM, 2020; Nappo et al., 2021).

Table 16.2 provides a comparison between the studies that, to the authors' knowledge, are currently using 3D models reconstructed from UAV images for road damage detection.

In the following, some technical requirements are given for optimizing the data quality.

Model georeferencing methods

Image data collected by UAV can be positioned and oriented in space by using direct or indirect georeferencing methods. This information is useful not only to georeference the final model in a global coordinate system but also to scale it.

Direct georeferencing adopts a GNSS receiver mounted onboard the UAV, working in code mode to obtain time and geolocation information with an accuracy of a few meters (Gabrlik, 2015), or in carrier-phase mode to reduce the error to a centimetric range (Colomina & Molina, 2014; Padró et al., 2019). These receivers can work with single or multi frequency using single (usually the GPS) or multiconstellation (GPS, GLONASS, GALILEO, and BEIDOU) systems. Moreover, two types of positioning can be distinguished: absolute, when only a receiver is boarded on the UAV that achieves an accuracy of meters; or differential (DGNSS), when a base station is on the ground (Giordan et al., 2020). In this latter case, time and geolocation information of UAV images can be processed after the flight via PPK (Padró et al., 2019; Rehak & Skaloud, 2017). An alternative to PPK is the RTK (Gabrlik, 2015; Padró et al., 2019) which allows the correction of the position estimated in real-time by applying the correction calculated and sent from a master receiver (located in a point of known coordinates) or a permanent station provided by a public institution, such as the virtual reference station networks (Giordan et al., 2020). The base-receivers are linked to the receiver onboard the UAV by radio, Bluetooth, or WLAN. The advantage of the postprocessing techniques is the available statistical information about the quality obtained in positioning.

Indirect georeferencing uses GCPs. GCPs are defined as points of known location and coordinates that can be easily recognized in the sequence of images acquired by UAV (Giordan et al., 2020). Typically, artificial black and white markers are preferred instead of natural elements of the scene (e.g., corners, artifacts, pedestrian crossing lines) because their color and geometry render them highly discernible in all images of the sequence (Caroti et al., 2015; Giordan et al., 2020). GCPs are placed in the surveyed area before the UAV

Table 16.2 Comparison between studies using UAV-based 3D models for road damage detection.

Road damage Type	Typical cause	UAV Flight altitude [m]	GSD [cm/pixel]	GCP	Georeferencing method	RMSE(x, y, z) [m]	Processing Data	Validation via field measurements	References
Block cracks	Shrinkage	5–7	0.64	Yes	GCP	–	3D point cloud	Yes	Inzerillo et al. (2018)
Longitudinal and transverse cracks	Landslide	10	0.37	No	Onboard GNSS	0.32, 0.61, 0.37	2D images and 3D point cloud	Yes	Nappo et al. (2021)
Rutting and potholes	Poor asphalt mixture	10–40	–	No	–	–	3D point cloud	Yes	Saad and Tahar (2019)
Potholes	Poor asphalt mixture	15	0.5	Yes	–	0.27–0.59, 0.23–0.53, 0.16–0.53	3D point cloud	Yes	Tan and Li (2019)

flight and used to improve the bundle adjustment (Caroti et al., 2015; Giordan et al., 2020), thus reaching errors in a centimeter range (Padró et al., 2019).

The use and the number of GCPs are particularly important to obtain highly accurate topographic models, as digital surface models (Caroti et al., 2015; Carvajal-Ramírez et al., 2016; Giordan et al., 2020; James et al., 2017; Martínez-Carricondo et al., 2018; Padró et al., 2019; Reshetyuk & Mårtensson, 2016; Santise et al., 2014; Tahar, 2013). Starting from a minimum of three, GCPs should be positioned either at the edges or inside the surveyed area with a stratified distribution to optimize both horizontal and vertical accuracy and minimize relative errors (Caroti et al., 2015; Giordan et al., 2020; James et al., 2017; Martínez-Carricondo et al., 2018; Tahar, 2013).

To define the most suitable georeferencing system for each application, it is important to evaluate the typology of the GNSS receiver, possible interferences (e.g., buildings, vegetation), and the accuracy that is required (Gabrlik, 2015; Giordan et al., 2020; Padró et al., 2019). If the objective of the study is the characterization and classification of asphalt pavement damage and the UAV is equipped with onboard bi-frequency GNSS receivers, GCPs can be theoretically omitted (Benassi et al., 2017; Gerke & Przybilla, 2016; Nappo et al., 2021; Nex et al., 2022). However, they can be used as support to estimate the position and scale error in the final model and they should be used in multitemporal analyses.

Data accuracy

The quality of UAV input images and output products (i.e., point cloud and orthophoto) depends on the intrinsic characteristics of the sensor, the flight mission, the photogrammetric processing, and the georeferencing system (Giordan et al., 2020; Martínez-Carricondo et al., 2018; Nex & Remondino, 2014; Santise et al., 2014; Tahar, 2013).

Sensor parameters that generally determine the quality of raw images are the camera focal length, exposure time, acquisition distortions, and pixel size. The flight altitude, speed, acquisition geometry (i.e., nadir or oblique), acquisition mode (e.g., manual or automatic) and ground sampling distance (GSD) affect the quality of either the raw images or the photogrammetric outputs (Agüera-Vega et al., 2017; Amrullah et al., 2016; Martínez-Carricondo et al., 2018; Mesas-Carrascosa et al., 2016). The flight speed should be determined according to the time exposure to avoid blurred images.

Additional environmental factors, such as wind speed, weather, morphology, and light/shadow conditions, influence the acquisition of UAV images and, consequently, the quality of UAV photogrammetric products (Dandois et al., 2015; Rock et al., 2011; Tahar, 2013). Photogrammetric products can be affected by errors in the raw input images, poor image overlap, presence/absence of GCPs, the georeferencing system, and the photogrammetric software (Caroti et al., 2015; Jaud et al., 2016;

Martínez-Carricondo et al., 2018; Murtiyoso & Grussenmeyer, 2017; Rosnell & Honkavaara, 2012; Tahar, 2013; Wierzbicki et al., 2015). In case the light/shadowing conditions are not optimal for the UAV survey, the images can be also pretreated with shadow removal algorithms (Nex & Remondino, 2014).

Pavement damage detection and classification using a UAV-integrated camera: a case study in North Italy

Nappo et al. (2021) developed a method for processing RGB images obtained by a UAV-based camera to measure the pavement damage in different landslide-affected roads and applied it to three different case studies in North Italy. After briefly describing the proposed method, the application to the provincial road SP14 in Laino municipality (North Italy) is discussed here.

Methodology

Fig. 16.1 illustrates the method proposed by (Nappo et al., 2021). Phase I consists in the acquisition from UAV of images of the investigated road section to be then processed via SfM to reconstruct a 3D point cloud and 2D orthophoto. Phase II is devoted to the point cloud processing. A planar reference surface is fitted to the road pavement to highlight the road pavement's unevenness. Then, certain geometric features, namely omnivariance, verticality, and roughness (Maas & Vosselman, 1999), are computed to automatically classify the 3D points into damage/nondamage and in four roughness levels (i.e., IRI) based on predetermined thresholds. In Phase III, the 2D orthophoto is processed via binarization and thresholding (Cubero-Fernandez et al., 2017), edge detection (Canny, 1986), and morphological operators to automatically extract damage polygons. These are then overlaid on the 3D point cloud to associate geometric (e.g., width and area) and photogrammetric (i.e., density of points, omnivariance, verticality, roughness) information to each crack and to classify the polygons according to their average roughness.

Results

Fig. 16.2 shows the photogrammetric products (i.e., 3D point cloud and 2D orthophoto) of the case-study road section SP14 in Laino municipality crossing an unstable slope with a rate of movement of a few millimeters per year. The slope is formed by Sinemurian—Lower Pliensbachian (Lower Jurassic) gray limestone in well-defined beds of 5–70 cm thickness and Late Pleistocene (Late Quaternary) glacial deposits in layers of 10–20 m of massive coarse gravels alternated with clayey silt and

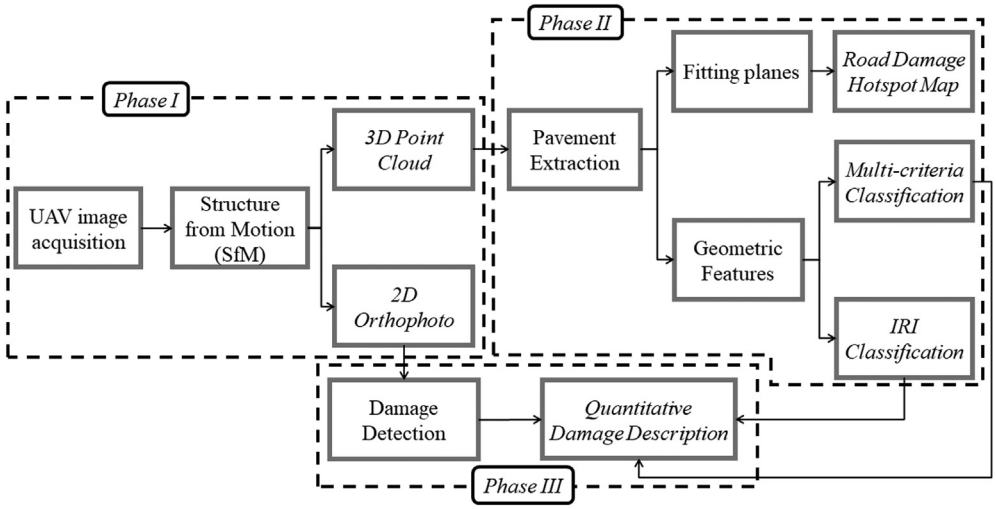

Figure 16.1 Flowchart for the assessment of road pavement damage. *Modified from Nappo, N., Mavrouli, O., Nex, F., van Westen, C., Gambillara, R., & Michetti, A. M. (2021). Use of UAV-based photogrammetry products for semi-automatic detection and classification of asphalt road damage in landslide-affected areas.* Engineering Geology, 294, *106363.* https://doi.org/10.1016/j.enggeo.2021.106363.

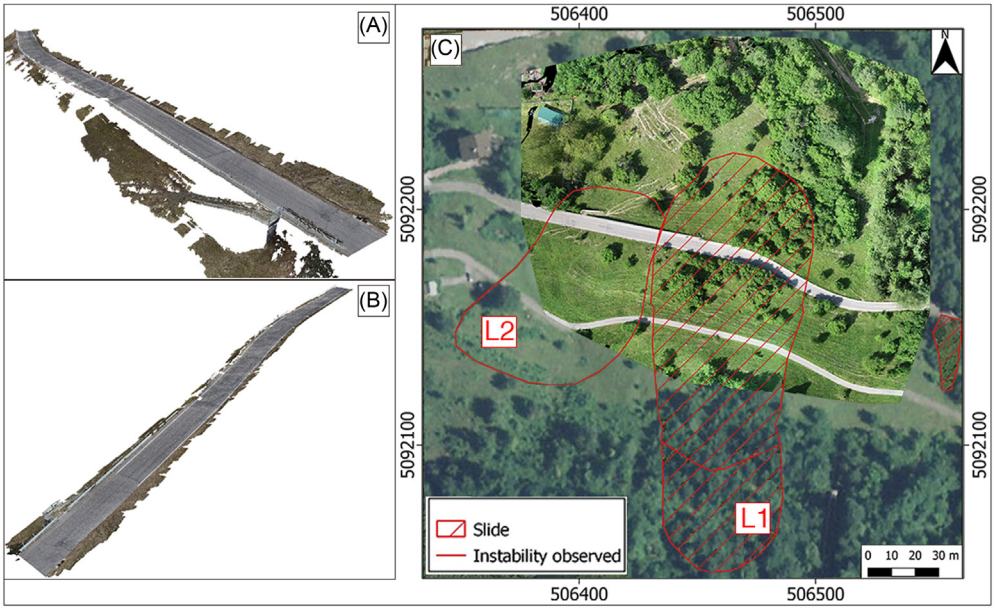

Figure 16.2 (A) and (B) 3D point cloud and (C) 2D orthophoto of the SP14 in Laino municipality crossing two landslides, as reconstructed via UAV-based SfM. Coordinates system: UTM 32 N (WGS84). *Modified from Nappo, N., Mavrouli, O., Nex, F., van Westen, C., Gambillara, R., & Michetti, A. M. (2021). Use of UAV-based photogrammetry products for semi-automatic detection and classification of asphalt road damage in landslide-affected areas.* Engineering Geology, 294, *106363.* https://doi.org/10.1016/j.enggeo.2021.106363.

limited sand (Bini et al., 1996; Michetti et al., 2014). The photogrammetric model of the road was reconstructed via SfM using 371 (5472 × 3078) RGB images of the SP14-Laino (toward the north in Fig. 16.2C) and 492 (5472 × 3078) RGB images of the entire area (Nappo et al., 2021).

The UAV survey was performed with a DJI Phantom 4 PRO flying at 10 m altitude from the main road and 30 m over the surrounding area. The images were acquired manually in nadir mode following a regular flight path assuring more than 80% overlap between adjacent images (Nappo et al., 2021). The bundle adjustment of the photogrammetric block was performed with SfM algorithms using commercial software (Nappo et al., 2021). Being the RMSE of the block adjustment lower than 0.7 m and the road section 200 m long, the relative error is acceptable for the average length of cracks and their width, and it did not affect the subsequent detection and classification of pavement damage. As mentioned, the section of the SP14-Laino shown in Fig. 16.3 is 200 m long and is characterized by 15 longitudinal cracks of 0.32–3.50 cm width and 8 transverse cracks of 0.76–2.63 cm, as measured during field investigations. A similar damage pattern was observed on a secondary road running upslope with respect to the SP14—Laino (Fig. 16.3), where additional 13 longitudinal and 9 transverse cracks were observed during field investigations.

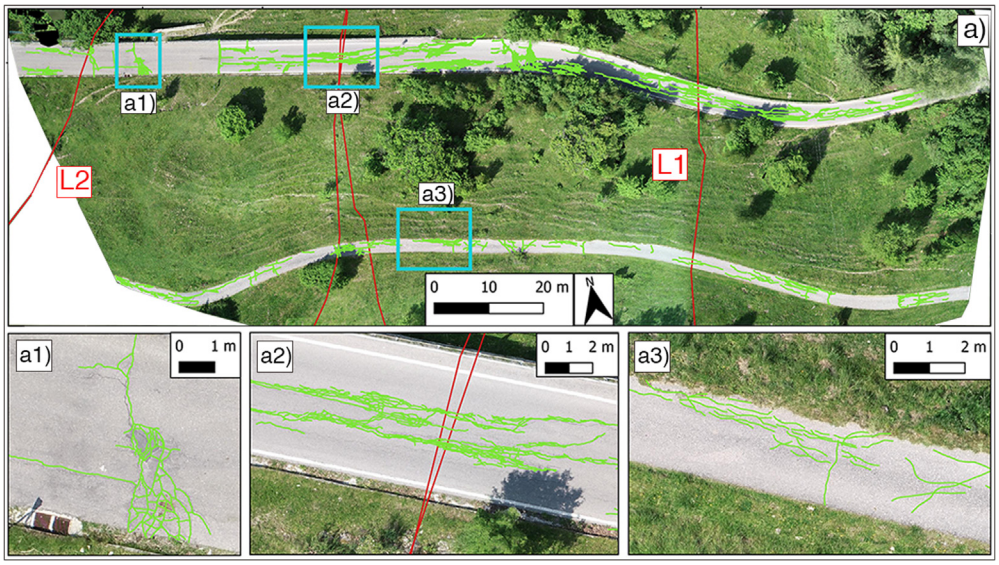

Figure 16.3 Evidence of longitudinal and transverse cracks on the pavement of the main road (towards north) and the secondary road running upslope (towards south). *Modified from Nappo, N., Mavrouli, O., Nex, F., van Westen, C., Gambillara, R., & Michetti, A. M. (2021). Use of UAV-based photogrammetry products for semi-automatic detection and classification of asphalt road damage in landslide-affected areas.* Engineering Geology, 294, *106363*. https://doi.org/10.1016/j.enggeo.2021.106363.

The authors performed a twofold analysis. First, they processed the 3D point cloud of the road section to retrieve a hotspot map of pavement unevenness (Fig. 16.4A) showing that heterogeneous landslide movements have resulted in irregular road damage patterns (Nappo et al., 2021). Then, they automatically classified the 3D points into damage/nondamage (Fig. 16.4b) and four severity levels based on the point roughness (i.e., IRI) (Fig. 16.4c). Afterward, the authors processed the 2D orthophoto of the SP14-Laino to automatically extract damage polygons that were classified according to their average roughness (i.e., IRI) (Fig. 16.4D). By combining the processing results of both UAV-based 2D orthophoto and 3D point clouds, the authors demonstrated that road pavement cracks wider than 1 cm can be detected. An overlap of 93% was found between automatic and manual damage detection (Nappo et al., 2021). The attributed damage classes are in accordance with visual observations.

Final remarks

The management of road infrastructure requires methodologies for quantitively assessing the damage induced by landslides on road asphalt pavements, other than the effects of usual stresses (AASHO, 1962; ANAS, 2004; ASTM, 2020).

The UAV products presented here have been proved to be successful in detecting landslide-induced longitudinal and transverse cracks. By processing the 2D images collected by digital cameras on a UAV platform, 3D point clouds and 2D orthophotos of the investigated road section can be generated. The three postprocessing products that can be provided following the procedure presented here are (1) a damage hotspot map to locate unevenness of the road pavement within the landslide body, (2) a 3D point cloud where points are attributed with a damage/nondamage value and a roughness value, and (3) locations of damage on the road in the form of damage polygons where the damage is classified according to the average roughness of the inside points. These products can assist in the prioritization of interventions and maintenance operations in a landslide risk management scenario.

It has been shown that UAV-based 3D models of road pavement can be used to automatically detect longitudinal and transverse cracks wider than 1 cm. This renders UAV-based camera sensors suitable for road damage assessment in the framework of vulnerability analyses, where quantitative parameters (e.g., road roughness) are needed to correlate the cause of damage (i.e., landslide) with its effect (i.e., different typologies of pavement cracks with different width and roughness). In this regard, the obtained models allow measuring the size (width, length, area), shape (pattern of points with similar features), the relative location of 3D points (distance from the reference plane, omnivariance, verticality), and roughness of longitudinal and transverse cracks on the road surface.

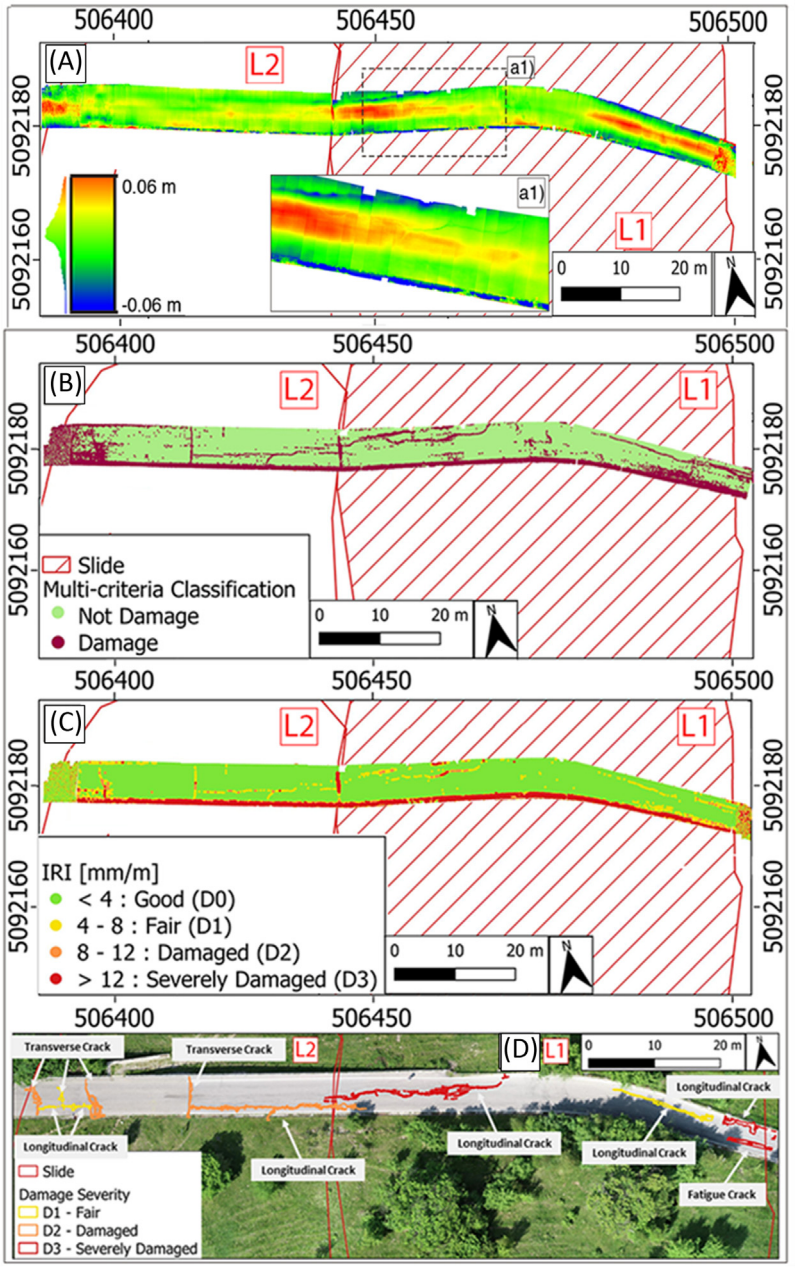

Figure 16.4 (A) Road damage hotspot map. Automatic classification of the 3D point cloud in (B) damage/nondamage and (C) IRI-based severity levels. (D) Classification of 2D road damage polygons in IRI-based severity levels. Coordinates system: UTM 32 N (WGS84). Map lines delineate study areas and do not necessarily depict accepted national boundaries. *Modified from Nappo, N., Mavrouli, O., Nex, F., van Westen, C., Gambillara, R., & Michetti, A. M. (2021). Use of UAV-based photogrammetry products for semi-automatic detection and classification of asphalt road damage in landslide-affected areas.* Engineering Geology, 294, *106363.* https://doi.org/10.1016/j.enggeo.2021.106363.

Compared to TLS and MLS, DP from UAV platforms has the advantage of acquiring data in complex topographic or morphological contexts with difficult access. Moreover, data acquired by UAVs are less sensitive to occlusion. Another advantage of using DP from UAV is the possibility of acquiring 2D image data to be used either for image analysis purposes or for reconstructing 3D models via the SfM algorithm. Nevertheless, precautions need to be taken during the acquisition and processing of the images. The UAV flight should be planned, thus determining the appropriate flight altitude (e.g., close or long range), speed, acquisition mode (i.e., nadir or oblique), GSD, minimum overlap between adjacent images (e.g., 80%), possibility of safely placing GCPs, presence of vegetation or other objects (e.g., power lines) that may obstruct the view and render the UAV flight unsafe. Depending on the length of the road section to be examined, the flight duration can be determined before the field survey, thus carrying an appropriate number of batteries, also depending on the UAV specifications, endurance, and capacity. The typology of the sensor to be used for road damage assessment can be determined based on the required GSD and resolution requirements of the images. At the time of writing, there is a variety of commercial models complying with the necessary prerequisites, such as a compact size and weight that allows to incorporate new sensors (e.g., digital camera, multiband camera, laser scanner), onboard GNSS receiver in single/multifrequency using single/multiple constellation with or without RTK options, and sufficient battery capacity to fly the UAV long enough to capture a multitude of information of the investigated target or area.

Given the difficulty in placing GCPs along road sections crossing steep unstable slopes, some authors neglect the use of GCPs for bundle adjustment or georeferencing of their 3D point clouds, opting instead for RTK georeferencing of each image based on the GNSS mounted onboard the UAV (Nappo et al., 2021; Saad & Tahar, 2019). This approach can generate a shift of the whole point cloud with respect to the datum, although not compromising the relative positioning of the UAV images and the road damage detection and measurement (Nappo et al., 2021; Nex et al., 2022). Nevertheless, to achieve high-accuracy, an adequate number of GCPs is required either at the edges or inside the surveyed scene (Caroti et al., 2015; James et al., 2017; Martínez-Carricondo et al., 2018; Tahar, 2013).

Future works may address a higher level of automation by implementing point pattern recognition of 3D points with similar features and applying artificial intelligence for road damage recognition and measurement (Nex et al., 2022). Additional efforts are needed to standardize the use of DP employing UAV platforms for road damage assessment in decision support systems for road maintenance agencies, such as the transportation asset management and pavement management system (Marzouk & Osama, 2017; Ragnoli et al., 2018; Sinha et al., 2017). Currently, DP from UAVs is suitable for small-scale investigations where national and international regulations permit it (EASA, 2022; ENAC, 2022; FAA, 2022; ICAO, 2022). These regulations often

require special permissions for operating UAVs for commercial or scientific purposes, thus preventing airspace congestion, preserving the privacy and safety of citizens, and assuring the safety of UAV operators and infrastructure users (Giordan et al., 2020). Nowadays, common international regulations have been established in Europe (EASA, 2022), for instance, to overcome the divergence of national laws. Despite the necessity of regulating the use of UAVs, especially to avoid their unsafe use, some authors (Giordan et al., 2020) argue that such restrictions are advisable in routine surveys but might be limited in emergency scenarios where quick responses are demanded (e.g., bridge collapse, sudden landslide activation, road blockage due to debris flows).

References

AASHO. (1962). *Road test-Report61E*. HRB, National Research Council.

ANAS. (2004). *Quaderni tecnici per la salvaguardia delle infrastrutture*. V.

ASTM. (2015). *Standard practice for computing international roughness index of roads from longitudinal profile measurements*. ASTM,

ASTM. (2020). *ASTM D6433-20 standard practice for roads and parking lots pavement condition index surveys*. ASTM International.

Achillopoulou, D. V., Mitoulis, S. A., Argyroudis, S. A., & Wang, Y. (2020). Monitoring of transport infrastructure exposed to multiple hazards: A roadmap for building resilience. *Science of the Total Environment*, *746*. Available from https://doi.org/10.1016/j.scitotenv.2020.141001, http://www.elsevier.com/locate/scitotenv.

Agüera-Vega, F., Carvajal-Ramírez, F., & Martínez-Carricondo, P. (2017). Assessment of photogrammetric mapping accuracy based on variation ground control points number using unmanned aerial vehicle. *Measurement*, *98*, 221–227. Available from https://doi.org/10.1016/j.measurement.2016.12.002.

Akgul, M., Yurtseven, H., Akburak, S., Demir, M., Cigizoglu, H. K., Ozturk, T., Eksi, M., & Akay, A. O. (2017). Short term monitoring of forest road pavement degradation using terrestrial laser scanning. *Measurement: Journal of the International Measurement Confederation*, *103*, 283–293. Available from https://doi.org/10.1016/j.measurement.2017.02.045.

Alhasan, A., White, D. J., & De Brabanter, K. (2017). Spatial pavement roughness from stationary laser scanning. *International Journal of Pavement Engineering*, *18*(1), 83–96. Available from https://doi.org/10.1080/10298436.2015.1065403, http://www.tandfonline.com/loi/gpav20.

Amrullah, C., Suwardhi, D., & Meilano, I. (2016). *ISPRS annals of the photogrammetry, remote sensing and spatial information sciences* (pp. 41–48). Copernicus GmbH, Indonesia. Available from https://doi.org/10.5194/isprs-annals-III-6-41-2016, http://www.isprs.org/publications/annals.aspx 3.

Anbazhagan, P., Srinivas, S., & Chandran, D. (2012). Classification of road damage due to earthquakes. *Natural Hazards*, *60*(2), 425–460. Available from https://doi.org/10.1007/s11069-011-0025-0.

Argyroudis, S. A., Mitoulis, S., Winter, M. G., & Kaynia, A. M. (2019). Fragility of transport assets exposed to multiple hazards: State-of-the-art review toward infrastructural resilience. *Reliability Engineering and System Safety*, *191*. Available from https://doi.org/10.1016/j.ress.2019.106567, https://www.journals.elsevier.com/reliability-engineering-and-system-safety.

Argyroudis, S. A., Mitoulis, S. A., Hofer, L., Zanini, M. A., Tubaldi, E., & Frangopol, D. M. (2020). Resilience assessment framework for critical infrastructure in a multihazard environment: Case study on transport assets. *Science of the Total Environment*, *714*. Available from https://doi.org/10.1016/j.scitotenv.2020.136854, http://www.elsevier.com/locate/scitotenv.

Argüelles-Fraga, R., Ordóñez, C., García-Cortés, S., & Roca-Pardiñas, J. (2013). Measurement planning for circular cross-section tunnels using terrestrial laser scanning. *Automation in Construction*, *31*, 1–9. Available from https://doi.org/10.1016/j.autcon.2012.11.023.

Barbarella, M., D'Amico, F., De Blasiis, M. R., Di Benedetto, A., & Fiani, M. (2018). Use of terrestrial laser scanner for rigid airport pavement management. *Sensors (Switzerland)*, *18*(1). Available from https://doi.org/10.3390/s18010044, http://www.mdpi.com/1424-8220/18/1/44/pdf.

Barbarella, M., De Blasiis, M. R., & Fiani, M. (2019). Terrestrial laser scanner for the analysis of airport pavement geometry. *International Journal of Pavement Engineering*, *20*(4), 466–480. Available from https://doi.org/10.1080/10298436.2017.1309194, http://www.tandfonline.com/loi/gpav20.

Benassi, F., Dall'Asta, E., Diotri, F., Forlani, G., Cella, U. Md, Roncella, R., & Santise, M. (2017). Testing accuracy and repeatability of UAV blocks oriented with gnss-supported aerial triangulation. MDPI AG, Italy. *Remote Sensing*, *9*(2). Available from https://doi.org/10.3390/rs9020172, http://www.mdpi.com/2072-4292/9/2/172/pdf.

Bini, A., Felber, M., Pomicino, N., & Zuccoli, L. (1996). Maximum extension of the glaciers (MEG) in the area comprised between Lago di Como, Lago Maggiore and their respective end-moraine system. *Geologia Insubrica*, *1*, 65–78.

Bryce, J., Boadi, R., & Groeger, J. (2019). Relating pavement condition index and present serviceability rating for asphalt-surfaced pavements. *Transportation Research Record*, *2673*(3), 308–312. Available from https://doi.org/10.1177/0361198119833671, http://journals.sagepub.com/home/trr.

Cahalane, C., Lewis, P., McElhinney, C. P., McNerney, E., & McCarthy, T. (2016). Improving MMS performance during infrastructure surveys through geometry aided design. *Infrastructures*, *1*(1). Available from https://doi.org/10.3390/infrastructures1010005, https://www.mdpi.com/2412-3811/1/1/5.

Canny, J. (1986). A computational approach to edge detection. *IEEE Transactions on Pattern Analysis and Machine Intelligence*, *PAMI-8*(6), 679–698. Available from https://doi.org/10.1109/tpami.1986.4767851.

Cardenal, J., Fernández, T., Pérez-García, J. L., & Gómez-López, J. M. (2019). Measurement of road surface deformation using images captured from UAVs. *Remote Sensing*, *11*(12). Available from https://doi.org/10.3390/rs11121507. https://res.mdpi.com/remotesensing/remotesensing-11-01507/article_deploy/remotesensing-11-01507-v2.pdf?filename = &attachment = 1.

Caroti, G., Martínez-Espejo Zaragoza, I. & Piemonte, A. (2015). *Accuracy assessment in structure from motion 3D reconstruction from UAV-born images: The influence of the data processing methods* (pp. 103–109). International Archives of the Photogrammetry, Remote Sensing and Spatial Information Sciences—ISPRS Archives. Italy: International Society for Photogrammetry and Remote Sensing. Available from https://doi.org/10.5194/isprsarchives-XL-1-W4-103-2015, http://www.isprs.org/proceedings/XXX>VIII/4-W15/ 40.

Carvajal-Ramírez, F., Agüera-Vega, F., & Martínez-Carricondo, P. J. (2016). Effects of image orientation and ground control points distribution on unmanned aerial vehicle photogrammetry projects on a road cut slope. *Journal of Applied Remote Sensing*, *10*(3), 034004. Available from https://doi.org/10.1117/1.jrs.10.034004.

Casagli, N., Frodella, W., Morelli, S., Tofani, V., Ciampalini, A., Intrieri, E., Raspini, F., Rossi, G., Tanteri, L., & Lu, P. (2017). Spaceborne, UAV and ground-based remote sensing techniques for landslide mapping, monitoring and early warning. *Geoenvironmental Disasters*, *4*(1). Available from https://doi.org/10.1186/s40677-017-0073-1, https://link.springer.com/journal/40677.

Chambon, S., & Moliard, J. M. (2011). Automatic road pavement assessment with image processing: Review and comparison. *International Journal of Geophysics*, *2011*. Available from https://doi.org/10.1155/2011/989354, http://www.hindawi.com/journals/ijgp/.

Chambon, S., Subirats, P., & Dumoulin, J. (2009). Introduction of a wavelet transform based on 2D matched filter in a Markov Random Field for fine structure extraction: Application on road crack detection. In *Proceedings of SPIE—The international society for optical engineering volume* 7251. France. Available from https://doi.org/10.1117/12.8054370277786X.

Chen, S., Laefer, D. F., Mangina, E., Zolanvari, S. M. I., & Byrne, J. (2019). UAV bridge inspection through evaluated 3D reconstructions. *Journal of Bridge Engineering*, *24*(4). Available from https://doi.org/10.1061/(ASCE)BE.1943-5592.0001343. http://ascelibrary.org/beo/resource/1/jbenf2.

Chin, A. (2012). Paving the way for terrestrial laser scanning assessment of road quality. Oregon State University.

Cigna, F., Banks, V. J., Donald, A. W., Donohue, S., Graham, C., Hughes, D., McKinley, J. M., & Parker, K. (2017). Mapping ground instability in areas of geotechnical infrastructure using satellite InSAR and

small UAV surveying: A case study in Northern Ireland. *Geosciences (Switzerland)*, *7*(3). Available from https://doi.org/10.3390/geosciences7030051, http://www.mdpi.com/2076-3263/7/3/51/pdf.

Coenen, T. B. J., & Golroo, A. (2017). A review on automated pavement distress detection methods. *Cogent Engineering*, *4*(1). Available from https://doi.org/10.1080/23311916.2017.1374822. http://www.tandfonline.com/toc/oaen20/current.

Colomina, I., & Molina, P. (2014). Unmanned aerial systems for photogrammetry and remote sensing: A review. *ISPRS Journal of Photogrammetry and Remote Sensing*, *92*, 79–97. Available from https://doi.org/10.1016/j.isprsjprs.2014.02.013, http://www.elsevier.com/inca/publications/store/5/0/3/3/4/0.

Crommelinck, S., Bennett, R., Gerke, M., Yang, M. Y., & Vosselman, G. (2017). Contour detection for UAV-based cadastral mapping. *Remote Sensing*, *9*(2). Available from https://doi.org/10.3390/rs9020171, http://www.mdpi.com/2072-4292/9/2/171/pdf.

Cubero-Fernandez, A., Rodriguez-Lozano, F. J., Villatoro, R., Olivares, J., & Palomares, J. M. (2017). Efficient pavement crack detection and classification. *Eurasip Journal on Image and Video Processing*, *2017*(1). Available from https://doi.org/10.1186/s13640-017-0187-0, http://www.springerlink.com/content/1687-5281/.

Dandois, J. P., Olano, M., & Ellis, E. C. (2015). Optimal altitude, overlap, and weather conditions for computer vision uav estimates of forest structure. *Remote Sensing*, *7*(10), 13895–13920. Available from https://doi.org/10.3390/rs71013895, http://www.mdpi.com/2072-4292/7/10/13895/pdf.

De Blasiis, M. R., Di Benedetto, A., & Fiani, M. (2020). Mobile laser scanning data for the evaluation of pavement surface distress. *Remote Sensing*, *2*(6). Available from https://doi.org/10.3390/rs12060942, https://res.mdpi.com/d_attachment/remotesensing/remotesensing-12-00942/article_deploy/remotesensing-12-00942-v2.pdf.

Donnini, M., Napolitano, E., Salvati, P., Ardizzone, F., Bucci, F., Fiorucci, F., Santangelo, M., Cardinali, M., & Guzzetti, F. (2017). Impact of event landslides on road networks: A statistical analysis of two Italian case studies. *Landslides*, *14*(4), 1521–1535. Available from https://doi.org/10.1007/s10346-017-0829-4, http://springerlink.metapress.com/app/home/journal.asp?wasp = e39xlqwvtg0yvw9n9h2m&referrer = parent&backto = browsepublicationsresults,328,541.

Díaz-Vilariño, L., González-Jorge, H., Bueno, M., Arias, P., & Puente, I. (2016). Automatic classification of urban pavements using mobile LiDAR data and roughness descriptors. *Construction and Building Materials*, *102*, 208–215. Available from https://doi.org/10.1016/j.conbuildmat.2015.10.199.

EASA. (2022). https://www.easa.europa.eu/domains/civil-drones.

ENAC. (2022). https://www.enac.gov.it/sicurezza-aerea/droni.

Elhadidy, A. A., El-Badawy, S. M., & Elbeltagi, E. E. (2021). A simplified pavement condition index regression model for pavement evaluation. *International Journal of Pavement Engineering*, *22*(5), 643–652. Available from https://doi.org/10.1080/10298436.2019.1633579, http://www.tandfonline.com/loi/gpav20.

FAA. (2022). https://www.faa.gov/uas/.

Fazio, N. L., Perrotti, M., Andriani, G. F., Mancini, F., Rossi, P., Castagnetti, C., & Lollino, P. (2019). A new methodological approach to assess the stability of discontinuous rocky cliffs using in-situ surveys supported by UAV-based techniques and 3-D finite element model: a case study. *Engineering Geology*, *260*. Available from https://doi.org/10.1016/j.enggeo.2019.105205, http://www.elsevier.com/inca/publications/store/5/0/3/3/3/0/.

Ferlisi, S., Marchese, A., & Peduto, D. (2021). Quantitative analysis of the risk to road networks exposed to slow-moving landslides: A case study in the Campania region (southern Italy. *Landslides*, *18*(1), 303–319. Available from https://doi.org/10.1007/s10346-020-01482-8, https://www.springer.com/journal/10346.

Fernandez Galarreta, J., Kerle, N., & Gerke, M. (2015). UAV-based urban structural damage assessment using object-based image analysis and semantic reasoning. *Natural Hazards and Earth System Sciences*, *15*(6), 1087–1101. Available from https://doi.org/10.5194/nhess-15-1087-2015, http://www.nat-hazards-earth-syst-sci.net/volumes_and_issues.html.

Fernández-Hernandez, J., González-Aguilera, D., Rodríguez-Gonzálvez, P., & Mancera-Taboada, J. (2015). Image-based modelling from unmanned aerial vehicle (UAV) photogrammetry: An effective, low-cost

tool for archaeological applications. *Archaeometry*, *57*(1), 128−145. Available from https://doi.org/10.1111/arcm.12078Spain, http://onlinelibrary.wiley.com/journal/10.1111/(ISSN)1475-4754.

Gabrlik, P. (2015). The use of direct georeferencing in aerial photogrammetry with micro UAV. *IFAC-PapersOnLine*, *48*, 380−385. Available from https://doi.org/10.1016/j.ifacol.2015.07.064 24058963 4. http://www.journals.elsevier.com/ifac-papersonline/ 28.

George, K. P., Rajagopal, A. S., & Lim, L. K. (1989). Models for predicting pavement deterioration. *Transportation Research Record*, *1215*, 1−7.

Gerke, M., & Przybilla, H. J. (2016). Accuracy analysis of photogrammetric UAV image blocks: Influence of onboard RTK-GNSS and cross flight patterns. *Photogrammetrie, Fernerkundung, Geoinformation*, *2016*(1), 17−30. Available from https://doi.org/10.1127/pfg/2016/0284, http://www.ingentaconnect.com/content/schweiz/pfg.

Gharaibeh, N. G., & Lindholm, D. (2014). A condition assessment method for roadside assets. *Structure and Infrastructure Engineering*, *10*(3), 409−418. Available from https://doi.org/10.1080/15732479.2012.757330.

Giordan, D., Adams, M. S., Aicardi, I., Alicandro, M., Allasia, P., Baldo, M., De Berardinis, P., Dominici, D., Godone, D., Hobbs, P., Lechner, V., Niedzielski, T., Piras, M., Rotilio, M., Salvini, R., Segor, V., Sotier, B., & Troilo, F. (2020). The use of unmanned aerial vehicles (UAVs) for engineering geology applications. *Bulletin of Engineering Geology and the Environment*, *79*(7), 3437−3481. Available from https://doi.org/10.1007/s10064-020-01766-2, http://link.springer.de/link/service/journals/10064/index.htm.

Gomez, C., & Purdie, H. (2016). UAV- based photogrammetry and geocomputing for hazards and disaster risk monitoring—A review. *Geoenvironmental Disasters*, *3*(1). Available from https://doi.org/10.1186/s40677-016-0060-y, https://link.springer.com/journal/40677.

Greenwood, W. W., Lynch, J. P., & Zekkos, D. (2019). Applications of UAVs in civil infrastructure. *Journal of Infrastructure Systems*, *25*(2). Available from https://doi.org/10.1061/(ASCE)IS.1943-555X.0000464.

Guan, H., Li, J., Yu, Y., Chapman, M., & Wang, C. (2015). Automated road information extraction from mobile laser scanning data. *IEEE Transactions on Intelligent Transportation Systems*, *16*(1), 194−205. Available from https://doi.org/10.1109/TITS.2014.2328589, http://ieeexplore.ieee.org/xpl/RecentIssue.jsp?punumber = 6979.

Guldur, B., Yan, Y., & Hajjar, J. F. (2015). Condition assessment of bridges using terrestrial laser scanners. In *Structures congress 2015—proceedings of the 2015 structures congress* (pp. 355−366). American Society of Civil Engineers (ASCE), United States. Available from https://doi.org/10.1061/9780784479117.031.

Hatmoko, J. U. D., Setiadji, B. H., Wibowo, M. A., Awaludin, A., Matsumoto, T., Pessiki, S., Jonkers, H., Siswosukarto, S., Setiawan, A. F., & Putri, K. N. R. (2019). Investigating causal factors of road damage: A case study. *MATEC Web of Conferences*, *258*, 02007. Available from https://doi.org/10.1051/matecconf/201925802007.

Holgado-Barco, A., Riveiro, B., González-Aguilera, D., & Arias, P. (2017). Automatic inventory of road cross-sections from mobile laser scanning system. *Computer-Aided Civil and Infrastructure Engineering*, *32*(1), 3−17. Available from https://doi.org/10.1111/mice.12213, http://www.blackwellpublishers.co.uk/journals/MICE/descript.htm.

ICAO (2022). 6. Available from https://www.icao.int.

Inzerillo, L., Di Mino, G., & Roberts, R. (2018). Image-based 3D reconstruction using traditional and UAV datasets for analysis of road pavement distress. *Automation in Construction*, *96*, 457−469. Available from https://doi.org/10.1016/j.autcon.2018.10.010.

James, M. R., Robson, S., d'Oleire-Oltmanns, S., & Niethammer, U. (2017). Optimising UAV topographic surveys processed with structure-from-motion: Ground control quality, quantity and bundle adjustment. *Geomorphology*, *280*, 51−66. Available from https://doi.org/10.1016/j.geomorph.2016.11.021, http://www.elsevier.com/inca/publications/store/5/0/3/3/3/4/.

Jaud, M., Passot, S., Bivic, R. L., Delacourt, C., Grandjean, P., & Dantec, N. L. (2016). Assessing the accuracy of high resolution digital surface models computed by PhotoScan® and MicMac® in sub-optimal survey conditions. *Remote Sensing*, *8*(6), 465. Available from https://doi.org/10.3390/rs8060465.

Kumar, P., & Angelats, E. (2017). An automated road roughness detection from mobile laser scanning data. In *International archives of the photogrammetry, remote sensing and spatial information sciences—ISPRS*

archives (pp. 91–96). International Society for Photogrammetry and Remote Sensing, Spain. Available from https://doi.org/10.5194/isprs-archives-XLII-1-W1-91-2017, http://www.isprs.org/proceedings/XXXVIII/4-W15/.

Kumar, P., Lewis, P., Mcelhinney, C. P., & Rahman, A. A. (2015). An algorithm for automated estimation of road roughness from mobile laser scanning data. *Photogrammetric Record*, *30*(149), 30–45. Available from https://doi.org/10.1111/phor.12090Malaysia, http://onlinelibrary.wiley.com/journal/10.1111/(ISSN)1477-9730.

Lei, B., Wang, N., Xu, P., & Song, G. (2018). New Crack detection method for bridge inspection using UAV incorporating image processing. *Journal of Aerospace Engineering*, *31*(5). Available from https://doi.org/10.1061/(ASCE)AS.1943-5525.0000879, http://ascelibrary.org/aso/resource/1/jaeeez.

Li, L., Luo, W., & Wang, K. C. P. (2018). Lane marking detection and reconstruction with line-scan imaging data. *Sensors (Switzerland)*, *18*(5). Available from https://doi.org/10.3390/s18051635, http://www.mdpi.com/1424-8220/18/5/1635/pdf.

Lissak, C., Bartsch, A., De Michele, M., Gomez, C., Maquaire, O., Raucoules, D., & Roulland, T. (2020). Remote sensing for assessing landslides and associated hazards. *Surveys in Geophysics*, *41*(6), 1391–1435. Available from https://doi.org/10.1007/s10712-020-09609-1, http://www.wkap.nl/journalhome.htm/0169-3298.

Liu, X., Wang, P., Lu, Z., Gao, K., Wang, H., Jiao, C., & Zhang, X. (2019). Damage detection and analysis of urban bridges using terrestrial laser scanning (TLS), ground-based microwave interferometry, and permanent scatterer interferometry synthetic aperture radar (PS-InSAR. *Remote Sensing*, *11* (5), 580. Available from https://doi.org/10.3390/rs11050580.

Lucieer, A., Jong, S. Md, & Turner, D. (2014). Mapping landslide displacements using Structure from Motion (SfM) and image correlation of multitemporal UAV photography. *Progress in Physical Geography*, *38*(1), 97–116. Available from https://doi.org/10.1177/0309133313515293, https://journals.sagepub.com/home/PPG.

Lõhmus, H., Ellmann, A., Märdla, S., & Idnurm, S. (2018). Terrestrial laser scanning for the monitoring of bridge load tests–two case studies. *Survey Review*, *50*(360), 270–284. Available from https://doi.org/10.1080/00396265.2016.1266117, http://www.tandfonline.com/loi/ysre20.

Maas, H. G., & Vosselman, G. (1999). Two algorithms for extracting building models from raw laser altimetry data. *ISPRS Journal of Photogrammetry and Remote Sensing*, *54*(2–3), 153–163. Available from https://doi.org/10.1016/S0924-2716(99)00004-0.

Macchiarulo, V., Milillo, P., Blenkinsopp, C., & Giardina, G. (2022). Monitoring deformations of infrastructure networks: A fully automated GIS integration and analysis of InSAR time-series. *Structural Health Monitoring*. Available from https://doi.org/10.1177/14759217211045912, http://shm.sagepub.com/.

Mancini, A., Malinverni, E. S., Frontoni, E., & Zingaretti, P. (2013). Road pavement crack automatic detection by MMS images. In *21st Mediterranean conference on control and automation, MED 2013—conference proceedings* (pp. 1589–1596). Italy Available from https://doi.org/10.1109/MED.2013.6608934.

Mandal, V., Uong, L., & Adu-Gyamfi, Y. (2019). Automated road crack detection using deep convolutional neural networks. In *Proceedings—2018 IEEE international conference on big data, big data 2018* (pp. 5212–5215). Seattle, WA: Institute of Electrical and Electronics Engineers Inc. Available from https://doi.org/10.1109/BigData.2018.8622327, http://ieeexplore.ieee.org/xpl/mostRecentIssue.jsp?punumber = 8610059.

Mansour, M. F., Morgenstern, N. R., & Martin, C. D. (2011). Expected damage from displacement of slow-moving slides. *Landslides*, *8*(1), 117–131. Available from https://doi.org/10.1007/s10346-010-0227-7.

Martínez-Carricondo, P., Agüera-Vega, F., Carvajal-Ramírez, F., Mesas-Carrascosa, F. J., García-Ferrer, A., & Pérez-Porras, F. J. (2018). Assessment of UAV-photogrammetric mapping accuracy based on variation of ground control points. *Journal of Applied Earth Observation and Geoinformation*, *72*, 1–10. Available from https://doi.org/10.1016/j.jag.2018.05.015, http://www.elsevier.com/locate/jag.

Marzouk, M., & Osama, A. (2017). Fuzzy-based methodology for integrated infrastructure asset management. *International Journal of Computational Intelligence Systems*, *10*(1), 745–759. Available from https://doi.org/10.2991/ijcis.2017.10.1.50, https://www.atlantis-press.com/journals/ijcis.

Mathavan, S., Rahman, M. M., Stonecliffe-Janes, M., & Kamal, K. (2014). Pavement raveling detection and measurement from synchronized intensity and range images. *Transportation Research Record*, *2457*, 3–11. Available from https://doi.org/10.3141/2457-01, http://trb.metapress.com/content/0361-1981/.

Mathavan, S., Rahman, M., & Kamal, K. (2015). Use of a self-organizing map for crack detection in highly textured pavement images. *Journal of Infrastructure Systems*, *21*(3). Available from https://doi.org/10.1061/(ASCE)IS.1943-555X.0000237, https://ascelibrary.org/journal/jitse4.

Mathavan, S., Kamal, K., & Rahman, M. (2015). A review of three-dimensional imaging technologies for pavement distress detection and measurements. *IEEE Transactions on Intelligent Transportation Systems*, *16*(5), 2353–2362. Available from https://doi.org/10.1109/TITS.2015.2428655, http://ieeexplore.ieee.org/xpl/RecentIssue.jsp?punumber = 6979.

Matsumoto, K., Arturo Linan Panting, C., Kitratporn, N., Takeuchi, W., Nagai, K., & Iwasaki, E. (2018). Performance assessment using structural analysis and spatial measurement of a damaged suspension bridge: Case study of Twantay Bridge, Myanmar. *Journal of Bridge Engineering*, *23*(10). Available from https://doi.org/10.1061/(ASCE)BE.1943-5592.0001293, http://ascelibrary.org/beo/resource/1/jbenf2.

Mavrouli, O., Corominas, J., Ibarbia, I., Alonso, N., Jugo, I., Ruiz, J., Luzuriaga, S., & Navarro, J. A. (2019). Integrated risk assessment due to slope instabilities in the roadway network of Gipuzkoa, Basque Country. *Natural Hazards and Earth System Sciences*, *19*(2), 399–419. Available from https://doi.org/10.5194/nhess-19-399-2019, http://www.nat-hazards-earth-syst-sci.net/volumes_and_issues.html.

Mertz, C. (2011). continuous road damage detection using regular service vehicles. *Proceedings ITS World Congress, Orlando*, 1–9.

Mesas-Carrascosa, F. J., García, M. D. N., Larriva., & García-Ferrer, A. (2016). An analysis of the influence of flight parameters in the generation of unmanned aerial vehicle (UAV) Orthomosaicks to survey archaeological areas. *Sensors*, *16*. Available from https://doi.org/10.3390/S16111838.

Michetti, A., Maria, L., Franz, P.' F., Vezzoli, L., Bini, A., Bernoulli, D., & Sciunnach, D. (2014). *Della Carta Geologica d'Italia*. Foglio 075, Como, Progetto CARG, 206. https://www.isprambiente.gov.it/Media/carg/75_COMO/Foglio.html.

Murtiyoso, A., & Grussenmeyer, P. (2017). Documentation of heritage buildings using close-range UAV images: dense matching issues, comparison and case studies. *Photogrammetric Record*, *32*(159), 206–229. Available from https://doi.org/10.1111/phor.12197, http://www.blackwellpublishing.com/journals/PhotRec.

Nappo, N., Peduto, D., Mavrouli, O., van Westen, C. J., & Gullà, G. (2019). Slow-moving landslides interacting with the road network: Analysis of damage using ancillary data, in situ surveys and multi-source monitoring data. Engineering Geology. 260, 105244. Available from https://doi.org/10.1016/j.enggeo.2019.105244.

Nappo, N., Mavrouli, O., Nex, F., Westen, C. van, Gambillara, R., & Michetti, A. M. (2021). Use of UAV-based photogrammetry products for semiautomatic detection and classification of asphalt road damage in landslide-affected areas. *Engineering Geology*, *294*, 106363. Available from https://doi.org/10.1016/j.enggeo.2021.106363.

Nex, F., & Remondino, F. (2014). UAV for 3D mapping applications: A review. *Applied Geomatics*, *6*(1), 1–15. Available from https://doi.org/10.1007/s12518-013-0120-x, http://www.springerlink.com/content/1866-9298/.

Nex, F., Duarte, D., Steenbeek, A., & Kerle, N. (2019). Towards real-time building damage mapping with low-cost UAV solutions. *Remote Sensing*, *11*(3). Available from https://doi.org/10.3390/rs11030287, https://www.mdpi.com/2072-4292/11/3/287/pdf.

Nex, F., Armenakis, C., Cramer, M., Cucci, D. A., Gerke, M., Honkavaara, E., Kukko, A., Persello, C., & Skaloud, J. (2022). UAV in the advent of the twenties: Where we stand and what is next. *ISPRS Journal of Photogrammetry and Remote Sensing*, *184*, 215–242. Available from https://doi.org/10.1016/j.isprsjprs.2021.12.006, http://www.elsevier.com/inca/publications/store/5/0/3/3/4/0.

Nhat-Duc, H., Nguyen, Q. L., & Tran, V. D. (2018). Automatic recognition of asphalt pavement cracks using metaheuristic optimized edge detection algorithms and convolution neural network. *Automation in Construction*, *94*, 203–213. Available from https://doi.org/10.1016/j.autcon.2018.07.008.

Niethammer, U., Rothmund, S., Schwaderer, U., Zeman, J., & Joswig, M. (2011). Open source image-processing tools for low-cost uav-based landslide investigations. *The International Archives of the Photogrammetry, Remote Sensing and Spatial Information Sciences*, *XXXVIII-1/C22*(1), 161–166. Available from https://doi.org/10.5194/isprsarchives-XXXviii-1-c22-161-2011.

Oguchi, T., Hayakawa, Y. S., & Wasklewicz, T. (2011). Data sources. *Developments in Earth Surface Processes*, *15*. Available from https://doi.org/10.1016/B978-0-444-53446-0.00007-0, http://www.elsevier.com/wps/find/bookdescription.cws_home/BS_DESP/description#description.

Oliveira, H., & Correia, P.L. (2009). Automatic road crack segmentation using entropy and image dynamic thresholding. In *European signal processing conference* (pp. 622–626). Portugal.

Oliveira, H., & Correia, P. L. (2013). Automatic road crack detection and characterization. *IEEE Transactions on Intelligent Transportation Systems*, *14*(1), 155–168. Available from https://doi.org/10.1109/TITS.2012.2208630.

Orellana, F., Blasco, J. M. D., Foumelis, M., D'aranno, P. J. V., Marsella, M. A., & Mascio, P. D. (2020). Dinsar for road infrastructure monitoring: Case study highway network of Rome metropolitan (Italy). *Remote Sensing*, *12*(22), 1–17. Available from https://doi.org/10.3390/rs12223697, https://www.mdpi.com/2072-4292/12/22/3697/pdf.

Ouyang, W., & Xu, B. (2013). Pavement cracking measurements using 3D laser-scan images. *Measurement Science and Technology*, *24*(10). Available from https://doi.org/10.1088/0957-0233/24/10/105204, http://iopscience.iop.org/0957-0233/24/10/105204/pdf/0957-0233_24_10_105204.pdf.

Padró, J. C., Muñoz, F. J., Planas, J., & Pons, X. (2019). Comparison of four UAV georeferencing methods for environmental monitoring purposes focusing on the combined use with airborne and satellite remote sensing platforms. *International Journal of Applied Earth Observation and Geoinformation*, *75*, 130–140. Available from https://doi.org/10.1016/j.jag.2018.10.018, http://www.elsevier.com/locate/jag.

Pagán, J. I., Bañón, L., López, I., Bañón, C., & Aragonés, L. (2019). Monitoring the dune-beach system of Guardamar del Segura (Spain) using UAV, SfM and GIS techniques. *Science of the Total Environment*, *687*, 1034–1045. Available from https://doi.org/10.1016/j.scitotenv.2019.06.186, http://www.elsevier.com/locate/scitotenv.

Pan, Y., Dong, Y., Wang, D., Chen, A., & Ye, Z. (2019). Three-dimensional reconstruction of structural surface model of heritage bridges using UAV-based photogrammetric point clouds. *Remote Sensing*, *11*(10), 1204. Available from https://doi.org/10.3390/rs11101204.

Pantelidis, L. (2011). A critical review of highway slope instability risk assessment systems. *Bulletin of Engineering Geology and the Environment*, *70*(3), 395–400. Available from https://doi.org/10.1007/s10064-010-0328-5.

Park, H. S., Lee, H. M., Adeli, H., & Lee, I. (2007). A new approach for health monitoring of structures: Terrestrial laser scanning. *Computer-Aided Civil and Infrastructure Engineering*, *22*(1), 19–30. Available from https://doi.org/10.1111/j.1467-8667.2006.00466.x.

Petrucci, O., & Gullà, G. (2010). A simplified method for assessing landslide damage indices. *Natural Hazards*, *52*(3), 539–560. Available from https://doi.org/10.1007/s11069-009-9398-8.

Ponzo, F.C., Iacovino, C., Ditommaso, R., Bonano, M., Lanari, R., Soldovieri, F., Cuomo, V., Bozzano, F., Ciampi, P., & Rompato, M. (2021). Transport infrastructure SHM using integrated SAR data and on-site vibrational acquisitions: "Ponte Della Musica–Armando Trovajoli" case study. *Applied Sciences, 11*, 6504.

Postance, B., Hillier, J., Dijkstra, T., & Dixon, N. (2017). Extending natural hazard impacts: An assessment of landslide disruptions on a national road transportation network. *Environmental Research Letters*, *12*(1). Available from https://doi.org/10.1088/1748-9326/aa5555, http://iopscience.iop.org/article/10.1088/1748-9326/aa5555/pdf.

Powell, L., & Satheeshkumar, K. G. (2017). Automated road distress detection. In *Proceedings of IEEE international conference on emerging technological trends in computing, communications and electrical engineering 2016*. India: ICETT. Institute of Electrical and Electronics Engineers Inc. Available from https://doi.org/10.1109/ICETT.2016.7873662 9781509037513.

Puan, O. C., Mustaffar, M., & Ling, T.-C. (2007). Automated pavement imaging program (APIP) For pavement cracks classification and quantification. *Malaysian Journal of Civil Engineering*, *19*.

Radopoulou, S.C., Brilakis, I., Doycheva, K., & Koch, C. (2016). A framework for automated pavement condition monitoring. In *Construction research congress 2016: Old and new construction technologies converge in historic San Juan—proceedings of the 2016* (pp. 770–779). United Kingdom: American Society of Civil Engineers (ASCE). Available from https://doi.org/10.1061/9780784479827.078 9780784479827.

Ragnoli, A., De Blasiis, M., & Di Benedetto, A. (2018). Pavement distress detection methods: A review. *Infrastructures*, *3*(4), 58. Available from https://doi.org/10.3390/infrastructures3040058.

Rehak, M., & Skaloud, J. (2017). Time synchronization of consumer cameras on Micro Aerial Vehicles. *ISPRS Journal of Photogrammetry and Remote Sensing*, *123*, 114–123. Available from https://doi.org/10.1016/j.isprsjprs.2016.11.009, http://www.elsevier.com/inca/publications/store/5/0/3/3/4/0.

Remondino, F., Nocerino, E., Toschi, I., & Menna, F. (2017). *A critical review of automated photogrammetric processing of large datasets* (pp. 591–599). International Archives of the Photogrammetry, Remote Sensing and Spatial Information Sciences—ISPRS Archives. Available from https://doi.org/10.5194/isprs-archives-XLII-2-W5-591-2017. 16821750 2. Italy: International Society for Photogrammetry and Remote Sensing. http://www.isprs.org/proceedings/XXXVIII/4-W15/ 42.

Reshetyuk, Y., & Mårtensson, S. G. (2016). Generation of highly accurate digital elevation models with unmanned aerial vehicles. *Photogrammetric Record*, *31*(154), 143–165. Available from https://doi.org/10.1111/phor.12143, http://www.blackwellpublishing.com/journals/PhotRec.

Rock, G., Ries, J. B., & Udelhoven, T. (2011). Sensitivity analysis of UAV-photogrammetry for creating digital elevation models (DEM. *The International Archives of the Photogrammetry, Remote Sensing and Spatial Information Sciences*, *XXXVIII-1/C22*(1), 69–73. Available from https://doi.org/10.5194/isprsarchives-XXXviii-1-c22-69-2011.

Rosnell, T., & Honkavaara, E. (2012). Point cloud generation from aerial image data acquired by a quadrocopter type micro unmanned aerial vehicle and a digital still camera. *Sensors*, *12*(1), 453–480. Available from https://doi.org/10.3390/s120100453Finland, http://www.mdpi.com/1424-8220/12/1/453/pdf.

Saad, A. M., & Tahar, K. N. (2019). Identification of rut and pothole by using multirotor unmanned aerial vehicle (UAV. *Measurement: Journal of the International Measurement Confederation*, *137*, 647–654. Available from https://doi.org/10.1016/j.measurement.2019.01.093.

Santise, M., Fornari, M., Forlani, G., & Roncella, R. (2014). *Evaluation of dem generation accuracy from UAS imagery* (pp. 529–536). International Archives of the Photogrammetry, Remote Sensing and Spatial Information Sciences—ISPRS Archives. Italy: International Society for Photogrammetry and Remote Sensing. Available from https://doi.org/10.5194/isprsarchives-XL-5-529-2014. 16821750 5. http://www.isprs.org/proceedings/XXXVIII/4-W15/ 40.

Schnebele, E., Tanyu, B. F., Cervone, G., & Waters, N. (2015). Review of remote sensing methodologies for pavement management and assessment. *European Transport Research Review*, *7*(2). Available from https://doi.org/10.1007/s12544-015-0156-6, http://www.springer.com/engineering/mechanical + eng/journal/12544.

Sedek, M., & Serwa, A. (2016). Development of new system for detection of bridges construction defects using terrestrial laser remote sensing technology. *Journal of Remote Sensing and Space Science*, *19*(2), 273–283. Available from https://doi.org/10.1016/j.ejrs.2015.12.005, http://www.elsevier.com/wps/find/journaldescription.cws_home/723780/description#description.

Sidess, A., Ravina, A., & Oged, E. (2021). A model for predicting the deterioration of the pavement condition index. *International Journal of Pavement Engineering*, *22*(13), 1625–1636. Available from https://doi.org/10.1080/10298436.2020.1714044, http://www.tandfonline.com/loi/gpav20.

Sinha, K. C., Labi, S., & Agbelie, B. R. D. K. (2017). Transportation infrastructure asset management in the new millennium: Continuing issues, and emerging challenges and opportunities. *Transportmetrica A: Transport Science*, *13*(7), 591–606. Available from https://doi.org/10.1080/23249935.2017.1308977, http://www.tandfonline.com/loi/ttra21?open = 8#vol_8.

Snavely, N., Seitz, S. M., & Szeliski, R. (2008). Modeling the world from internet photo collections. *International Journal of Computer Vision*, *80*(2), 189–210. Available from https://doi.org/10.1007/s11263-007-0107-3.

Stumpf, A., Malet, J. P., Kerle, N., Niethammer, U., & Rothmund, S. (2013). Image-based mapping of surface fissures for the investigation of landslide dynamics. *Geomorphology*, *186*, 12–27. Available from https://doi.org/10.1016/j.geomorph.2012.12.010.

Tahar, K. N. (2013). An evaluation on different number of ground control points in unmanned aerial vehicle photogrammetric block. *The International Archives of the Photogrammetry, Remote Sensing and Spatial Information Sciences*, *XL-2/W2*, 93–98. Available from https://doi.org/10.5194/isprsarchives-xl-2-w2-93-2013.

Tan, Y., & Li, Y. (2019). UAV photogrammetry-based 3D road distress detection. *ISPRS International Journal of Geo-Information*, *8*(9). Available from https://doi.org/10.3390/ijgi8090409, https://www.mdpi.com/2220-9964/8/9.

Uddin, W. (2014). Remote sensing laser survey and imagery technologies for expediting airport mapping and asset management applications. *International Journal of Roads and Airports*, *1*, 53–67.

Valença, J., Puente, I., Júlio, E., González-Jorge, H., & Arias-Sánchez, P. (2017). Assessment of cracks on concrete bridges using image processing supported by laser scanning survey. *Construction and Building Materials*, *146*, 668–678. Available from https://doi.org/10.1016/j.conbuildmat.2017.04.096.

Van Der Horst, B. B. Lindenbergh, R. C., & Puister, S. W. J. (2019). *Mobile laser scan data for road surface damage detection* (pp. 1141–1148). International Archives of the Photogrammetry, Remote Sensing and Spatial Information Sciences—ISPRS Archives. Netherlands: International Society for Photogrammetry and Remote Sensing. Available from https://doi.org/10.5194/isprs-archives-XLII-2-W13-1141-2019, http://www.isprs.org/proceedings/XXXVIII/4-W15/.

Vasuki, Y., Holden, E. J., Kovesi, P., & Micklethwaite, S. (2014). Semi-automatic mapping of geological Structures using UAV-based photogrammetric data: An image analysis approach. *Computers and Geosciences*, *69*, 22–32. Available from https://doi.org/10.1016/j.cageo.2014.04.012, http://www.elsevier.com/inca/publications/store/3/9/8/.

Vetrivel, A., Gerke, M., Kerle, N., Nex, F., & Vosselman, G. (2018). Disaster damage detection through synergistic use of deep learning and 3D point cloud features derived from very high resolution oblique aerial images, and multiple-kernel-learning. *ISPRS Journal of Photogrammetry and Remote Sensing*, *140*, 45–59. Available from https://doi.org/10.1016/j.isprsjprs.2017.03.001, http://www.elsevier.com/inca/publications/store/5/0/3/3/4/0.

Vosselman, G., & Maas, H. G. (2010). *Airborne and terres-trial laser scanning*. Whittles Publishing.

Wang, K.C. P., & Gong, W. (2002). Automated pavement distress survey: A review and a new direction. ICC MDR408X View project pavement texture.

Wang, K. C. P., & Li, X. (1999). Use of digital cameras for pavement surface distress survey. *Transportation Research Record*, *1675*, 91–97. Available from https://doi.org/10.3141/1675-12.

Wang, W., Wang, M., Li, H., Zhao, H., Wang, K., He, C., Wang, J., Zheng, S., & Chen, J. (2019). Pavement crack image acquisition methods and crack extraction algorithms: A review. *Journal of Traffic and Transportation Engineering (English Edition)*, *6*(6), 535–556. Available from https://doi.org/10.1016/j.jtte.2019.10.001, http://www.journals.elsevier.com/journal-of-traffic-and-transportation-engineering-english-edition.

Westoby, M. J., Brasington, J., Glasser, N. F., Hambrey, M. J., & Reynolds, J. M. (2012). 'Structure-from-Motion' photogrammetry: A low-cost, effective tool for geoscience applications. *Geomorphology*, *179*, 300–314. Available from https://doi.org/10.1016/j.geomorph.2012.08.021.

Wierzbicki, D., Kedzierski, M., & Fryskowska, A. (2015). *Assesment of the influence of UAV image quality on the orthophoto production* (Vol. XL-1/W4, pp. 1–8). International archives of the photogrammetry, remote sensing and spatial information sciences—ISPRS archives. Poland: International Society for Photogrammetry and Remote Sensing. Available from https://doi.org/10.5194/isprsarchives-XL-1-W4-1-2015, 168217501. http://www.isprs.org/proceedings/XXXVIII/4-W15/ 40.

Williams, K., Olsen, M. J., Roe, G. V., & Glennie, C. (2013). Synthesis of transportation applications of mobile LIDAR. *Remote Sensing*, *5*(9), 4652–4692. Available from https://doi.org/10.3390/rs5094652United, http://www.mdpi.com/2072-4292/5/9/4652/pdf.

Winter, M. G. (2019). Laboratory investigation of the impact force of debris flow on a passable structure. In *The XVII European conference on soil mechanics and geotechnical engineering*. Reykjavík, Iceland 1–6 September 2019. Available from https://doi.org/10.32075/17ECSMGE-2019-1118.

Winter, M. G., Smith, J. T., Fotopoulou, S., Pitilakis, K., Mavrouli, O., Corominas, J., & Agyroudis, S. (2013) The physical vulnerability of roads to debris flow. In *18th international conference on soil mechanics*

and geotechnical engineering: Challenges and innovations in geotechnics (pp. 2281–2284). United Kingdom: IOS Press. http://www.cfms-sols.org/actes-du-colloque?lang = en 3.

Winter, M. G., Shearer, B., Palmer, D., Peeling, D., Harmer, C., & Sharpe, J. (2016). The Economic impact of landslides and floods on the road network. *Procedia Engineering*, *143*, 1425–1434. Available from https://doi.org/10.1016/j.proeng.2016.06.168, http://www.sciencedirect.com/science/journal/18777058.

Zakeri, H., Nejad, F. M., & Fahimifar, A. (2017). Image based techniques for crack detection, classification and quantification in asphalt pavement: A review. *Archives of Computational Methods in Engineering*, *24*(4), 935–977. Available from https://doi.org/10.1007/s11831-016-9194-z, http://www.springerlink.com/content/1134-3060.

Zhang, W., & Wang, M. L. (2018). International roughness index (IRI) measurement using hilbert-huang transform. In *Proceedings of SPIE—the international society for optical engineering*. Available from https://doi.org/10.1117/12.2297211, http://spie.org/x1848.xml 10599.

Zou, Q., Cao, Y., Li, Q., Mao, Q., & Wang, S. (2012). CrackTree: Automatic crack detection from pavement images. *Pattern Recognition Letters*, *33*(3), 227–238. Available from https://doi.org/10.1016/j.patrec.2011.11.004.